Mon. Not. R. astr. Soc. (1971) **152,** 307–322.

ON THE CAUSE OF THE NOVA OUTBURST

Sumner Starrfield

(Received 1971 January 8)

SUMMARY

The observational studies of the old novae have shown that they are close binaries with one of the components a white dwarf accreting hydrogen-rich material from the other component. To determine if the nova outburst could be caused by a thermal runaway in the envelope of the white dwarf, a computer code designed to take short time steps has been used to compute evolutionary sequences for helium-rich white dwarfs with hydrogen-rich envelopes. None of those computed using initial conditions derived from the observations of DQ Her had significant thermal runaways or produced the 10^{45} erg observed in the outburst of DQ Her. An evolutionary sequence was then computed which used initial conditions that included the effects of an accretion shock (Starrfield 1970). A thermal runaway resulted which produced the energy observed in the outburst of DQ Her.

Two evolutionary sequences were computed with a mass of $0{\cdot}5\ M_{\odot}$. A thermal runaway occurred in each sequence and produced more than 10^{45} erg. In these models as the peak of the runaway was reached, the shell source compressed and heated the outer layers of the helium core until helium burning was initiated.

1. INTRODUCTION

Over the last few years intensive observational studies of the old novae have shown that an old nova is a close binary consisting of a large, cool star filling its Lagrangian lobe and a smaller hotter star which is most likely a bright white dwarf. In addition, these studies (Kraft 1963, 1964; Paczynski 1965b; Mumford 1967) suggest that the larger, cooler star is losing hydrogen-rich material and that a fraction of this material is being accreted by the hotter star. As the accretion continues, a layer of hydrogen-rich material will be built up on the surface of the hot star and the bottom of this layer will be gradually compressed and heated until it reaches the ignition temperature for the hydrogen-burning reactions. If the nova outburst actually occurs on the hotter star (hereafter assumed to be a white dwarf) it must be determined if such a process will result in a thermal runaway that can produce the 10^{45} erg observed in an outburst.

Of major concern to this explanation of the nova outburst is the determination that the outbursts of the common novae actually occur on the white dwarf. Krzeminski (1965) has shown that in U Gem, a dwarf nova, the outburst occurs on the cooler star. However, Walker & Chincarini (1968) have observed SS Cyg, also a dwarf nova, and find that the outbursts occur on the white dwarf. Smak (1969) has re-analysed their data and finds that it is quite likely that the outbursts occur, instead, on the cooler star in this system. Paczynski (1965a) and Bath (1969) have studied close binaries and find that a star with a convective envelope filling its Lagrangian lobe is unstable to expansion on a dynamical time scale. Their results can explain the outburst in a dwarf nova but the energy liberated by their models is

a factor of 10^4 to 10^6 smaller than what is observed in a common nova outburst. It must be assumed that another process is acting in the common novae.

Accretion of hydrogen-rich material onto a white dwarf was first considered by Mestel (1952) who was trying to explain the supernovae. He used a model where $2{\cdot}5 \times 10^{29}$ g had been accreted by a star whose internal temperature was very high ($T > 10^8$ °K). A thermal runaway occurred and produced about 10^{49} erg. However, he neglected accretion heating which would raise the hydrogen-rich layers to thermonuclear temperatures long before this much material had been accreted. In addition, Schatzman (1965) argued that since the material at the bottom of the envelope was completely degenerate, the electron conductivity would circulate the energy throughout the interior and the reactions would die out. Saslaw (1968) reconsidered Mestel's work and included the heating due to accretion. His thermal runaways were not as violent as Mestel's and did not produce the total energy observed in the nova outburst. In addition, his zero boundary assumptions break down near the peak of the outburst when convection is important. Convection will cause more of the envelope to be included in the energy producing region and increase the amount of energy produced by nuclear reactions.

More detailed models of white dwarfs accreting hydrogen have been computed by Giannone & Weigert (1967) and Rose (1968). Rose studied the onset of pulsational instability in a $0{\cdot}75\ M_\odot$ white dwarf accreting hydrogen-rich material. He showed that a thermal runaway would occur but his chosen luminosity was much too high and the thermal runaway occurred before enough material had been accreted to produce the observed energy. Giannone & Weigert (1967, hereafter GW) studied the evolution of two $0{\cdot}5\ M_\odot$ white dwarfs of much lower luminosity than Rose. They also produced a thermal runaway but were forced to stop their integrations long before the peak because of numerical difficulties.

The present investigation is a study of the development of the thermal runaway in the hydrogen-rich envelope of a helium-rich white dwarf, coming as close as possible to the peak of the outburst using a hydrostatic stellar evolution program. This program was designed to take time steps as short as minutes. Two masses were considered: $0{\cdot}12\ M_\odot$, to study the evolution of DQ Her; and $0{\cdot}5\ M_\odot$, to compare the present work with GW and also determine the effect of mass on the development of the thermal runaway.

2. MODEL CONSTRUCTION

(a) *Basic equations*

The evolutionary sequences were calculated by means of a hydrostatic, semi-implicit, time-dependent computer code that included both convective and radiative energy transport. Because of the need to take extremely short time steps, the entropy was considered to be the fundamental variable. The change in entropy was obtained from the energy conservation equation written in the form

$$dS = \left(\frac{\epsilon_{\text{nuc}}}{T} - \frac{1}{T}\frac{\partial L}{\partial m}\right) dt. \tag{1}$$

The luminosity gradient was obtained by a numerical differentiation of the temperature gradient. The hydrostatic structure was then calculated by using the stepwise method (Schwarzschild 1958). The inner boundary was treated as a hard

core at $q \approx 0{\cdot}95$ with constant radius and luminosity. The outer boundary condition was obtained from a grid of envelopes using the triangle procedure as described by Kippenhahn, Weigart & Hofmeister (1967). The intermediate region was divided into 50 to 60 mass zones containing from 10^{23} g at the surface to 10^{30} g at the inner boundary. The small mass shells at the surface limited the time step to 5×10^4 s. This was because round-off and truncation error in the computer produced a spurious luminosity gradient in the outermost shells. The resulting entropy changes had to be kept small or the iterations would not converge. A secant procedure was used to accelerate the convergence of the iterations in each time step.

The radiative opacity is obtained from Cox & Stewart (1965); the Kippenhahn II ($x = 0{\cdot}900$, $y = 0{\cdot}099$, $z = 0{\cdot}001$) composition was used for the hydrogen-rich envelope; and the Weigert IV ($x = 0{\cdot}000$, $y = 0{\cdot}999$, $z = 0{\cdot}001$) composition was used for the helium-rich core. The degenerate electron conductivity was obtained from Lee (1950) as described in Schatzman (1958). These conductivities are larger than the more accurate values of Hubbard & Lampe (1969) by about a factor of two. This implies that the importance of electron conduction in shutting off the thermal runaway by carrying heat into the interior has been overestimated. However, in none of the models does electron conduction become important.

The gas is assumed to be completely ionized (partial ionization is included near the surface) and the pressure due to the partially degenerate electrons is included by means of a table of $P/\rho^{5/3}$ as a function of $V\eta(1/2)$, where

$$V\eta(1/2) = \frac{1}{\Gamma\left(\frac{5}{2}\right)} \int_0^\infty \frac{x^{1/2}\,dx}{e^{x-\eta}+1} \tag{2}$$

(Tolman 1938). The envelope does not extend down to depths where relativistic degeneracy is important and it is not included.

The hydrogen burning reactions have been included in the form given by Iben (1965). Since the carbon cycle predominates during the important stages of the evolution, recent corrections to the proton–proton cycle have not been included. Helium burning reaction rates were obtained from Reeves (1965). The change in hydrogen abundance during the evolution was calculated and included in the computations. In addition, all convective regions in the interior were assumed to be in adiabatic equilibrium.

(b) *Initial model*

The program used to compute the initial model for each evolutionary sequence is a standard, step-wise, stellar envelope code which computes a stellar envelope model for a given mass, luminosity, and effective temperature. The program includes the mixing-length theory (Böhm-Vitense 1958) in the form described by Kippenhahn, *et al.* (1967). The thermodynamic parameters needed for the calculation are obtained from the procedure described in Baker & Kippenhahn (1962). The opacity and equation of state subroutines are identical to those in the time-dependent code. This program is also used to compute the envelope grid used as the outer boundary condition in the time-dependent program.

The initial model of each evolutionary sequence is computed by integrating a model envelope with the hydrogen-rich composition from the surface to a given depth and then changing to the helium-rich composition and integrating inwards to

the hard core. Hydrogen burning reactions are neglected in the first model even though the hydrogen-rich material may extend to depths where the temperature is more than 20 million degrees.

(*c*) *Comparison with Giannone & Weigert* (1967)

Table I shows a comparison at two different depths of two computations of pure helium envelopes using the same luminosity and effective temperature. The largest difference occurs at the surface where GW assumed the zero boundary conditions. In fact, a significant super-adiabatic convective region exists near the surface of the model and is caused by the partial ionization of He I and He II. As the depth increases this region becomes adiabatic and convection extends to depths of 5×10^5 °K and a mass of 4×10^{22} g. The existence of a convective region probably invalidates the time scale of the $0{\cdot}5\ M_\odot$ evolutionary sequence that GW computed without mass accretion. The agreement at the deeper point is good, the small difference is due in part to a difference in composition. GW used $x = 0{\cdot}000$, $y = 0{\cdot}956$, $z = 0{\cdot}444$ for their model.

TABLE I

Comparisons of two helium-rich model envelopes at two depths

Depth		log r	log P	log ρ	log T	log M*
1	GW†	9·051	14·097	−0·045	6·354	28·0
	P.W.‡	9·050	13·878	−0·045	6·124	25·0
2	GW	9·018	18·627	3·548	7·107	30·0
	P.W.	9·020	18·620	3·530	7·133	30·0

* Mass in grams overlying this depth.
† Giannone & Weigert (1967).
‡ Present Work.

TABLE II

Comparison of two evolutionary sequences

	Time ≈ 0			Time ≈ 3×10^5 years		
	log ρ_{tr}*	log T_{tr}	log M_{tr}	log ρ_{tr}	log T_{tr}	log M_{tr}
GW	3·088	7·124	29·776	2·793	7·73	30·104
P.W.	3·133	7·108	29·795	2·40	7·74	29·795

* ' tr ' stands for the hydrogen–helium composition interface.

It is more important to compare the results of our two different evolutionary sequences. Table II shows the density and temperature at the beginning of the nuclear burning phase and again 3×10^5 years later. The second point is the last one given by GW. The much larger decrease in density in the present work is caused by our neglect of accretion. Part of the intent in the construction of this model was a minimum outburst, so it had only half the mass in the envelope as the corresponding model of GW. This model continued to evolve for another 62 days. At this time the temperature and density at the hydrogen–helium interface (the peak of the shell source) are log $T_{tr} = 8{\cdot}08$ and log $\rho_{tr} = 1{\cdot}37$. The rate of energy generation has increased to 2×10^{11} erg g^{-1} s^{-1}, 10^{46} erg have been produced from nuclear reactions, 5×10^{38} erg s^{-1} are flowing out of the shell source, and helium burning

has begun in the helium-rich layer just below the hydrogen–helium interface (a more detailed discussion of the evolution of this model can be found in Section 4).

(d) Including the effects of accretion

While the effect of the accretion is not explicitly included in the program, it is still possible to make an order-of-magnitude estimate of its relative importance to the evolutionary models. Kippenhahn, Thomas & Weigert (1965) have shown that the Second Law of Thermodynamics can be written in the form:

$$\frac{dS}{dt} = C_p \left(\frac{\dot{T}}{T} - \nabla_{AD} \frac{\dot{P}}{P}\right). \tag{3}$$

To arrive at expressions for the change in temperature and pressure at the hydrogen–helium interface produced by the accretion of more mass onto the star, one integrates the equations of stellar structure and assumes the zero-boundary conditions and Kramer's opacity (Schwarzschild 1958):

$$T_{tr} = \left[\frac{1}{4{\cdot}25} \frac{H\mu}{k} G\right] M \left(\frac{1}{r} - \frac{1}{R}\right) \tag{4}$$

and

$$P_{tr} = \left[\frac{2}{8{\cdot}5} \frac{4ac}{3} \frac{k}{H} \frac{4\pi G}{\mu\kappa_0}\right]^{1/2} \left(\frac{M}{L}\right)^{1/2} T_{tr}^{4{\cdot}25}. \tag{5}$$

Taking the logarithmic derivative of these two equations and substituting the result into (3), one finds that with $\nabla_{AD} = 0{\cdot}4$

$$\frac{dS_{tr}}{dt} = C_p \left[0{\cdot}2 \frac{\dot{L}}{L} - 0{\cdot}9 \frac{\dot{M}}{M} - 0{\cdot}7\eta\right], \tag{6}$$

where

$$\eta = \left(\frac{1}{R^2} \dot{R} - \frac{1}{r^2} \dot{r}\right) \cdot \frac{Rr}{R-r}. \tag{7}$$

The calculations of GW show that for a $0{\cdot}5\ M_\odot$ star: $\dot{R}/R \approx 1000\dot{M}/M$, $\dot{r}/r \approx \dot{M}/M$, and $\dot{L}/L$ is a very strongly varying function of $\dot{M}/M$. A rough mean of their results is $\dot{L}/L \approx 1500\ \dot{M}/M$. Therefore, η has the value of about $5 \times 10^2\ s^{-1}$. For an assumed value of $\dot{M}$ of $10^{-8}\ M_\odot\ yr^{-1}$ (Starrfield 1970), dS_{tr}/dt has the value: -6×10^{-6}. Since S_{tr} is 2×10^9 erg g^{-1} $°K^{-1}$, it will take $\approx 10^8$ years for accretion to affect the entropy at the hydrogen–helium interface. The value of dS_{tr}/dt for $0{\cdot}12\ M_\odot$ is not as certain since evolutionary calculations similar to GW are not available, but dS/dt is probably of the same order of magnitude. The foregoing result agrees with the evolutionary calculations of GW who obtained a strong peak in the temperature at the hydrogen–helium interface. Until hydrogen burning was initiated, the temperature and density increased nearly adiabatically. Therefore, by integrating the initial model to a greater depth and higher temperature and density, it is possible to partially compensate for not including accretion. The rise in the temperature of the transition zone caused by the accretion is a very strong function of the rate of accretion. In fact, at $0{\cdot}5\ M_\odot$, $\dot{T}_{tr}/T_{tr} \approx 500\dot{M}/M$.

3. THE PRE-OUTBURST EVOLUTION OF DQ HER

(a) *The initial model*

It has recently been proposed that the high luminosity of the white dwarf component of DQ Her is due to an accretion shock front at the stellar surface (Starrfield 1970). In the first part of this section further evidence for this proposal will be presented. This evidence consists of the results of a series of evolutionary sequences computed for DQ Her that used observationally-determined luminosities and effective temperatures. Fig. 1 shows the luminosities and effective temperatures

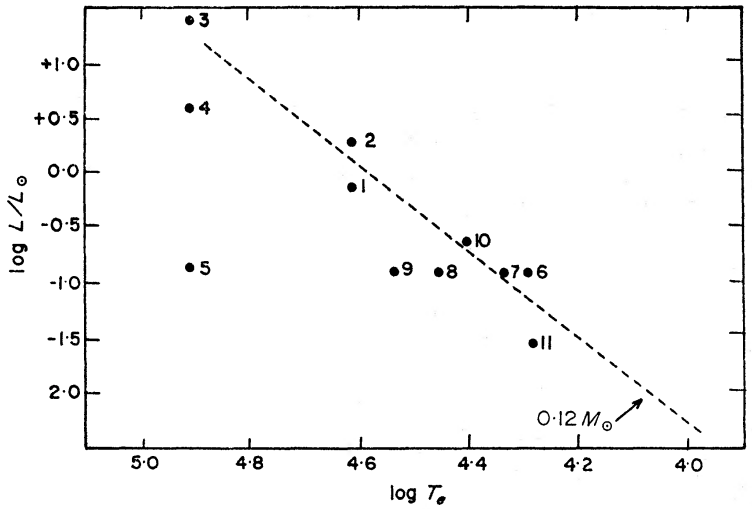

FIG. 1. *The location of the initial models of the evolutionary sequences for DQ Her. The values of luminosity and effective temperature were chosen from the observations and the origin of each value is described in the text. The dashed line is the constant radius line for a zero-temperature, pure helium, white dwarf with a mass of* $0{\cdot}12 M_{\odot}$. *The mass–radius relation is from Hamada & Salpeter* (1961).

of the various initial models plotted in the HR diagram. The characteristics of each model can be found in Table III. In some cases only the luminosity, effective temperature, or radius was obtained from the literature; the other parameters were chosen arbitrarily to provide a reasonable spread of the models over the white dwarf region of the HR diagram.

Models 1 and 2 use the electron temperature and M_v from Kraft (1959) and bolometric corrections for white dwarfs from Matsushima & Terashita (1969). Models 3, 4 and 5 use the 80 000°K effective temperature from Kraft (1959); and in addition, models 3 and 4 use radii given in his paper, while model 5 uses the value of M_{Bol} given by Mumford (1967). Models 6, 7, 8 and 9 use M_{Bol} from Mumford (1967) and an arbitrary series of effective temperatures. Model 10 uses the Hamada & Salpeter (1961) mass–radius relation for pure helium white dwarfs and the effective temperature was chosen to be 25 000°K. Model 11 was chosen as a comparison with the $0{\cdot}5\ M_{\odot}$ Model of GW.

The results of the evolution of these models can be found also in Table III. They are quite conclusive in that none of these models produced the energy observed in a common nova outburst. The evolution of these models was carried past the peak of the thermal runaway to where it was clear that the runaway has levelled off and was declining. In addition, many of these models are physically

TABLE III

Models for DQ Her with initial conditions derived from the observations

Model	$\log L/L_\odot$	$\log T_e$	$\log R$ (cm)	M_{tr}* ($\times 10^{28}$ g)	$\log r_{tr}$ (cm)	$\log T_{tr}$ (°K)	$\log \rho_{tr}$ (g cm^{-3})	$\log \epsilon_{max}$† erg^{-1} g^{-1} s^{-1}	E_{tot}‡ erg	$\log R_{end}$§ cm
1	−0·15	4·602	9·08	4·9	8·85	7·136	1·901	2·72	1·E36	9·13
2	+0·25	4·602	9·28	6·6	8·97	7·109	1·528	1·76	1·E32	9·34
3	1·370	4·903	9·24	0·83	8·95	7·132	0·712	—	—	—
4	0·576	4·903	8·84	0·273	8·70	7·119	1·320	4·63	4·E36	9·00
5	−0·934	4·903	8·08	0·007	8·06	7·112	2·353	12·00	4·E40	8·53
6	−0·90	4·290	9·32	49·3	8·99	7·100	2·293	3·34	2·E39	9·57
7	−0·90	4·330	9·24	22·1	8·98	7·037	2·093	3·01	1·E38	9·50
8	−0·90	4·450	9·01	9·46	8·81	7·124	2·371	5·64	2·E40	9·36
9	−0·90	4·530	8·84	1·76	8·72	7·044	2·118	5·97	8·E39	9·17
10	−0·65	4·398	9·24	25·9	8·93	7·134	2·241	3·63	6·E37	9·37
11	−1·507	4·281	9·04	28·0	8·82	7·117	2·731	5·20	2·E41	9·23

* Mass overlying the hydrogen–helium composition interface indicated by ' tr '.
† Maximum rate at which energy is produced in the model.
‡ Total amount of energy produced in the evolution.
§ Radius of final model of each sequence.

unrealistic since they lie below the line of constant radius for a zero-temperature white dwarf with a mass of $0{\cdot}12\ M_{\odot}$.

The luminosities and effective temperatures chosen for the initial models are those characteristic of the flow of energy from the interior. If those parameters chosen from the observations do not provide us with realistic models, then criteria must be developed that will result in realistic models. Therefore, a grid of model envelopes (the initial model code was used) was constructed for $0{\cdot}12M_{\odot}$, $0{\cdot}3\ M_{\odot}$, and $0{\cdot}5\ M_{\odot}$ using the hydrogen-rich composition. Each envelope was integrated in depth until a constant *temperature* of 12·6 million degrees was reached. At this depth the physical parameters describing the model were tabulated: the density, pressure, radius, mass of the material overlying this depth ($M_{\rm tr}$), and $V\eta(1/2)$ the degree of degeneracy. Lines of constant $M_{\rm tr}$ in the HR diagram have been plotted in Fig. 2

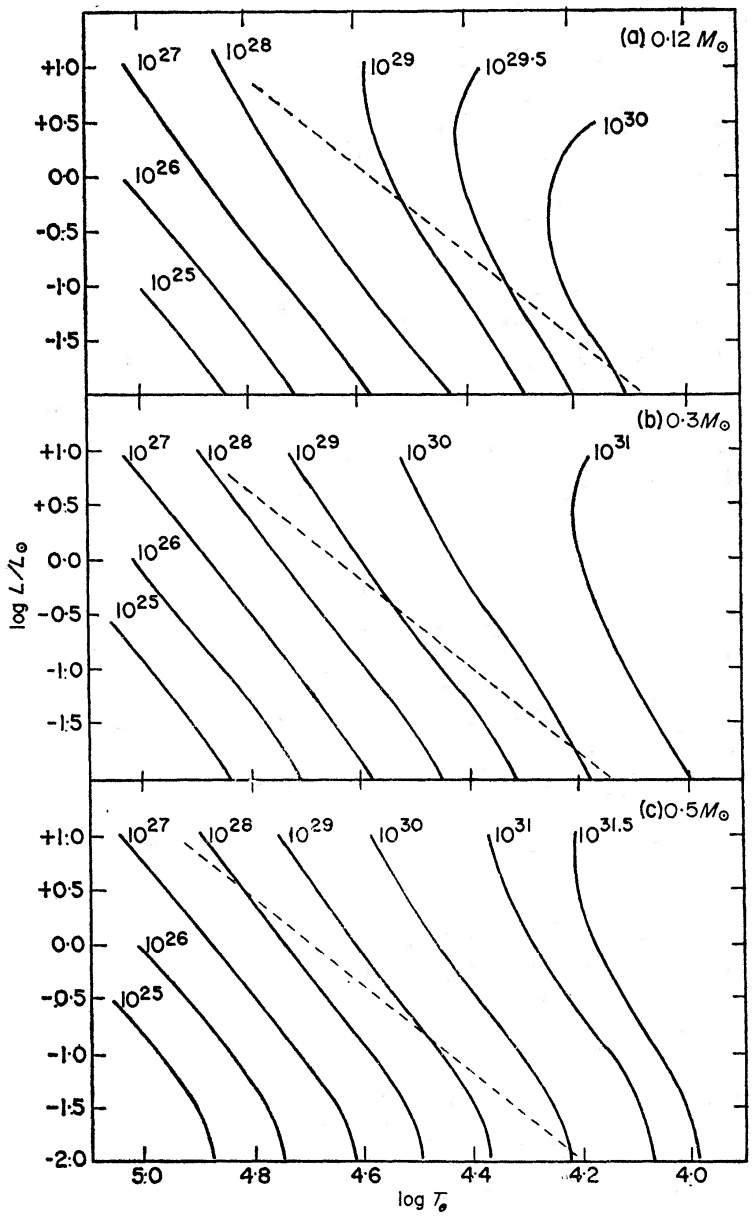

FIG. 2. *Lines of constant mass (g) overlying the depth where the temperature reaches* $12{\cdot}6 \times 10^{6}$°*K. The total mass used to compute each plot is indicated in the upper right-hand corner. The dashed line is the constant radius line for a white dwarf of the given mass.*

for the three masses. The dashed line in each plot is the constant radius line for a white dwarf of the given mass computed by means of the Hamada & Salpeter (1961) mass–radius relation for pure helium, zero-temperature, white dwarfs. The region of the HR diagram below this line is forbidden to any white dwarf with a mass of $0{\cdot}12\ M_\odot$ or less.

The radiative energy liberated during the outburst of DQ Her amounted to 10^{45} erg and more than 2×10^{28} g were ejected with a kinetic energy of 2×10^{43} erg (Payne–Gaposchkin & Gaposchkin 1942). Hazelhurst (1962) has calculated that only one per cent of the energy liberated in the interior will appear as kinetic energy of the expanding gas. This result has been confirmed by the numerical study of Sparks (1969). This means that at least 2×10^{45} erg must have been produced in the interior of DQ Her. If all this energy comes from the conversion of hydrogen to helium, then 10^{27} g of hydrogen are needed to produce the energy released during the outburst. The results of the evolutionary calculations show that less than 0·1 per cent of the available hydrogen is burnt during the outburst, and therefore, 10^{30} g of hydrogen-rich material are needed in the envelope. Referring to Fig. 2 (a), a $0{\cdot}12\ M_\odot$ white dwarf with 10^{30} g of hydrogen-rich material in its envelope has to have a luminosity less than $0{\cdot}01\ L_\odot$ and an effective temperature less than 15 000 °K.

Although the shell source in the final models is thin enough to satisfy the Schwarzschild & Härm (1965) conditions for a non-degenerate thermal runaway and the layer is initially unstable, the layers above the shell source will be able to expand fast enough to quickly cool the runaway if the shell source is not partially degenerate. This phenomenon is what occurred in the models discussed previously. Table IV shows the run of $\log V\eta(1/2)_{\rm tr}$ tabulated at a constant depth of 12·6 million

TABLE IV

Variation of $\log V\eta(1/2)_{\rm tr}$ *as a function of* $\log L/L_\odot$ *for* $0{\cdot}12M_\odot$, $0{\cdot}3M_\odot$, *and* $0{\cdot}5M_\odot$

	$\log V\eta(1/2)_{\rm tr}$		
$\log L/L_\odot$	$0{\cdot}12M_\odot$	$0{\cdot}3M_\odot$	$0{\cdot}5M_\odot$
+1·0	−1·66	−1·34	−1·20
+0·5	−1·26	−0·98	−0·84
+0·0	−0·90	−0·63	−0·49
−0·5	−0·55	−0·30	−0·17
−1·0	−0·22	0·02	0·15
−1·5	0·09	0·34	0·50
−2·0	0·42	0·75	1·07

Note: $\log V\eta(1/2)$ is not a function of $T_{\rm eff}$ (see text). The degenerate electron pressure and perfect-gas electron pressure are equal at $\log V\eta(1/2) = 0{\cdot}473$.

degrees. It is obtained from the envelope grid mentioned previously. $V\eta(1/2)_{\rm tr}$ is independent of effective temperature since it varies as $P_{\rm tr}/T_{\rm tr}^{5/2}$ and equation (5) shows that for a constant mass and temperature $P_{\rm tr}$ varies only as the luminosity. The value of $\log V\eta(1/2)$ at which the pressure of the degenerate electrons is equal to the perfect gas electron pressure is 0·473. If one requires that the bottom of the hydrogen envelope be at least this degenerate, then Table IV shows that the models are again limited to low luminosities and effective temperatures.

Recent studies of DQ Her suggest that the radius of the white dwarf may be smaller, and hence the mass larger, than predicted from the 71-second pulsation

period (Nather & Warner 1969). This is not surprising since the calculations (Skilling 1968) assumed a zero-temperature white dwarf. A thick non-degenerate envelope will lengthen the period for a given mass. Therefore, Fig. 2 also shows plots of constant M_{tr} for $0{\cdot}3M_{\odot}$ and $0{\cdot}5\ M_{\odot}$. These graphs show that one is still forced to pick lower luminosities and effective temperatures for the initial models than one would predict from the observations.

(*b*) *Realistic models for DQ Herculis*

The criteria of the preceding section were used to choose an initial model with a luminosity of $\log L/L_{\odot} = -1{\cdot}9$ and an effective temperature of $\log T_e = 4{\cdot}05$. The compressional heating of the envelope was included by moving the luminosity and effective temperature along a line in the HR diagram parallel to the evolutionary track of GW and then integrating in depth to higher temperatures. This procedure resulted in a model with $\log L/L_{\odot} = -1{\cdot}25$, $\log T_e = 4{\cdot}25$. This model had a hydrogen rich shell with $2{\cdot}84 \times 10^{30}$ g extending to depths where the temperature was 24 million degrees and the density was $3{\cdot}2 \times 10^3$ g cm^{-3}.*

TABLE V

The evolution of the shell source

at $0{\cdot}12M_{\odot}$ $\log L/L_{\odot} = -1{\cdot}25$ $\log T_e = 4{\cdot}25$

Time (days)	log T	log ρ	log ϵ_{nuc}	log L	log R	log S	X_H	X_{He4}
			Shell 39					
−138 (yr)	7·381	3·506	5·640	32·270	8·796	9·438	0·900	0·099
−2·72 (yr)	7·655	2·678	8·276	34·473	8·834	9·496	0·893	0·106
34·3	7·682	2·594	8·499	35·050	8·833	9·502	0·893	0·106
57·3	7·688	2·593	8·558	35·106	8·831	9·503	0·893	0·106
80·4	7·696	2·597	8·670	35·188	8·825	9·503	0·893	0·106
92·9	7·715	2·617	8·908	35·384	8·811	9·504	0·893	0·106
			Shell 40					
−138 (yr)	7·245	4·086	0·0	−31·597	8·728	8·997	0·00	0·999
−2·72 (yr)	7·273	4·126	0·0	−31·696	8·724	8·997	0·0	0·999
34·3	7·470	4·422	0·0	−32·943	8·693	8·997	0·0	0·999
57·3	7·507	4·478	0·0	−33·370	8·686	8·997	0·0	0·999
80·4	7·572	4·575	0·0	−33·972	8·674	8·997	0·0	0·999
92·9	7·696	4·761	0·0	−35·032	8·650	8·997	0·0	0·999

The evolution of the shell source is presented in Table V. After 135 years of evolution, the radius of the model increased from $8{\cdot}8 \times 10^3$ km to 26×10^3 km. Very soon after the initiation of nuclear burning, a convective region formed at the shell source and slowly worked its way outwards extending from a radius of $6{\cdot}4 \times 10^3$ km to $15{\cdot}8 \times 10^3$ km. The formation and growth of a convective region agrees with the calculations of GW, Rose (1968), and Sparks (1969).

After another 80 days of evolution, the total radius is 34×10^3 km while the convective region has grown to 32×10^3 km. For about the last 70 days, the gradually increasing strength of the shell source has caused the outer layers of the helium core

* At a mass accretion rate of $10^{-8}\ M_{\odot}$ yr^{-1} (Starrfield 1970), it would take DQ Her about 140 000 years to accrete this much material and this would raise the temperatures to 24×10^6 °K. So a time step of about 10^5 years has been implicitly assumed.

to be compressed. This is shown in Fig. 3. This core compression occurred in all the realistic models in this study as they approached the peak of the outburst. Although the velocity of the helium core just below the shell source has only reached -100 cm s^{-1}, at the last time step the model tries to rebound dynamically and the evolution is ended. This evolutionary sequence has produced 2×10^{45} erg from nuclear reactions and the shell source is currently producing 10^{40} erg s^{-1}.

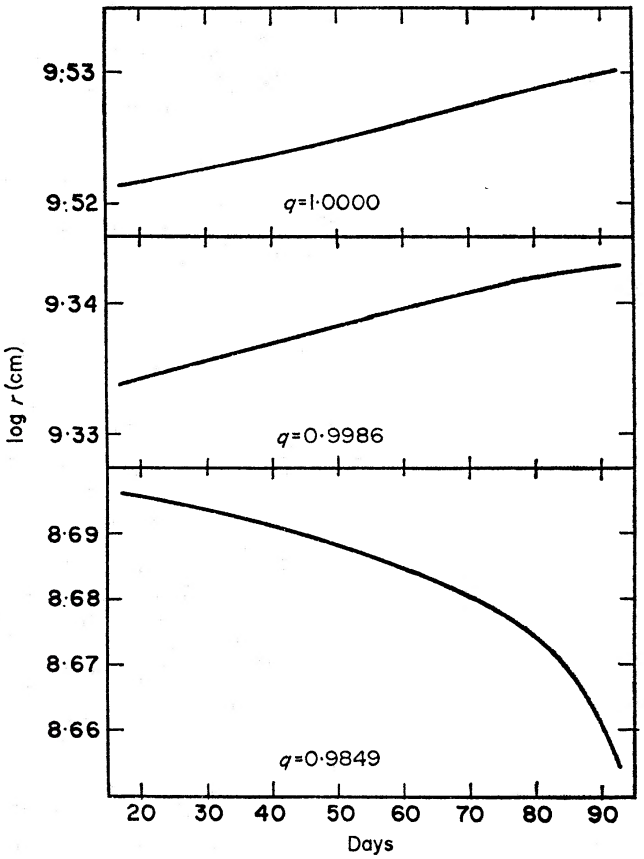

FIG. 3. *Radius as a function of time for three shells from the* $0{\cdot}12 M_\odot$, $\log L/L_\odot = -1{\cdot}25$, $\log T_e = 4{\cdot}25$, *evolutionary sequence. Note that the time of evolution is much longer than that of the* $0{\cdot}5 M_\odot$ *evolutionary sequences.*

4. EVOLUTION AT $0{\cdot}5\ M_\odot$

(a) *The initial models*

A grid of model envelopes extending to 12·6 million degrees was also constructed for $0{\cdot}5\ M_\odot$. Fig. 2 (c) shows the curves of constant M_{tr} for this mass. Comparing Figs 2 (a) and 2 (c), it can be seen that a $0{\cdot}5 M_\odot$ equilibrium model can have a larger luminosity and effective temperature than the $0{\cdot}12\ M_\odot$ model with the same value of M_{tr}. Moreover, the $0{\cdot}5\ M_\odot$ evolutionary sequences show that one per cent of the available hydrogen, rather than the tenth of a per cent at $0{\cdot}12\ M_\odot$, is burned during the evolution, lowering the mass cut-off to 10^{29} g. The degeneracy cut-off also occurs at a higher luminosity (*cf.* Table IV).

Two evolutionary sequences were computed for $0{\cdot}5\ M_\odot$. The first one was characterized by $\log L/L_\odot = -1{\cdot}507$, $\log T_e = 4{\cdot}281$ and has already been mentioned in a previous section. It was chosen to have the minimal conditions for a nova outburst. The second sequence, characterized by $\log L/L_\odot = -1{\cdot}210$,

$\log T_e = 4{\cdot}343$, represents a more evolved white dwarf that has accreted a factor of three more hydrogen-rich material than the other $0{\cdot}5\ M_\odot$ model. It represents the other extreme of the nova and should have a more violent outburst.

(b) $\log L/L_\odot = -1{\cdot}507$, $\log T_e = 4{\cdot}281$

Heating by accretion is not included and the model took 3×10^5 years to reach the time of the outburst. The evolution of the shell source is presented in Table VI. A convective region formed just above the shell source after about 10^5 years of evolution and gradually moved outwards as the strength of the shell source increased. Five days before the peak of the outburst was reached, the entire hydrogen-rich envelope became convective.

TABLE VI

Evolution of the shell source at

$0{\cdot}5M_\odot$ $\log L/L_\odot = -1{\cdot}507$ $\log T_e = 4{\cdot}281$

Shell 37

Time (days)	log T	log ρ	log ϵ_{nuc}	log L	log r	log S	X_H	X_{He4}
−2·8E5 (yr)	7·108	3·133	2·162	32·072	8·979	9·432	0·9000	0·0990
+4·25	7·816	2·264	9·656	36·242	9·002	9·527	0·8900	0·1090
31·5	7·873	2·125	10·114	36·556	9·010	9·538	0·8900	0·1090
38·1	7·899	2·051	10·299	36·701	9·015	9·543	0·8899	0·1091
44·8	7·933	1·936	10·521	36·903	9·024	9·550	0·8898	0·1092
51·5	7·976	1·746	10·733	37·176	9·041	9·561	0·8895	0·1095
55·7	8·001	1·580	10·800	37·349	9·060	9·570	0·8893	0·1097
59·5	8·020	1·426	10·816	37·777	9·078	9·577	0·8890	0·1100
62·0	8·060	1·347	11·098	38·593	9·072	9·583	0·8889	0·1101
62·1	8·079	1·368	11·288	38·715	9·059	9·583	0·8889	0·1101
				Shell 38				
−2·8E5 (yr)	7·145	3·609	0·0	32·101	8·974	9·012	0·0	0·999
+4·25	7·085	3·520	0·0	−32·675	8·976	9·012	0·0	0·999
31·5	7·073	3·502	0·0	−32·598	8·977	9·012	0·0	0·999
38·1	7·068	3·494	0·0	−32·549	8·977	9·012	0·0	0·999
44·8	7·063	3·486	0·0	−32·462	8·977	9·012	0·0	0·999
51·5	7·072	3·500	0·0	−32·280	8·977	9·012	0·0	0·999
55·7	7·123	3·577	0·0	−31·768	8·975	9·012	0·0	0·999
59·5	7·280	3·811	0·0	−33·040	8·968	9·012	0·0	0·999
62·0	7·930	4·636	−0·615	−39·024	8·928	9·019	0·0	0·999
62·1	8·054	5·048	5·319	+38·054	8·908	9·008	0·0	0·999

During its evolution, this model liberated $2{\cdot}7 \times 10^{46}$ erg from nuclear reactions. Most of the energy is produced in the last ten days of the evolution. This sequence also exhibits the core compression found in the $0{\cdot}12\ M_\odot$ evolution (see Fig. 4). However, the inward velocity of the outermost shell of the helium core is more than a factor of 10 greater than in the $0{\cdot}12\ M_\odot$ model; it reached a maximum of -2×10^3 cm s^{-1}. A few hours before the peak is reached, core compression reached the point where the temperature and density was high enough to initiate helium burning in the outer edges of the core. As the strength of the helium burning shell increased, it slowed down and halted the core compression. At this point the evolution is ended. During the last few hours before the peak is reached, the model is producing about 10^{44} erg hr^{-1} from nuclear reactions.

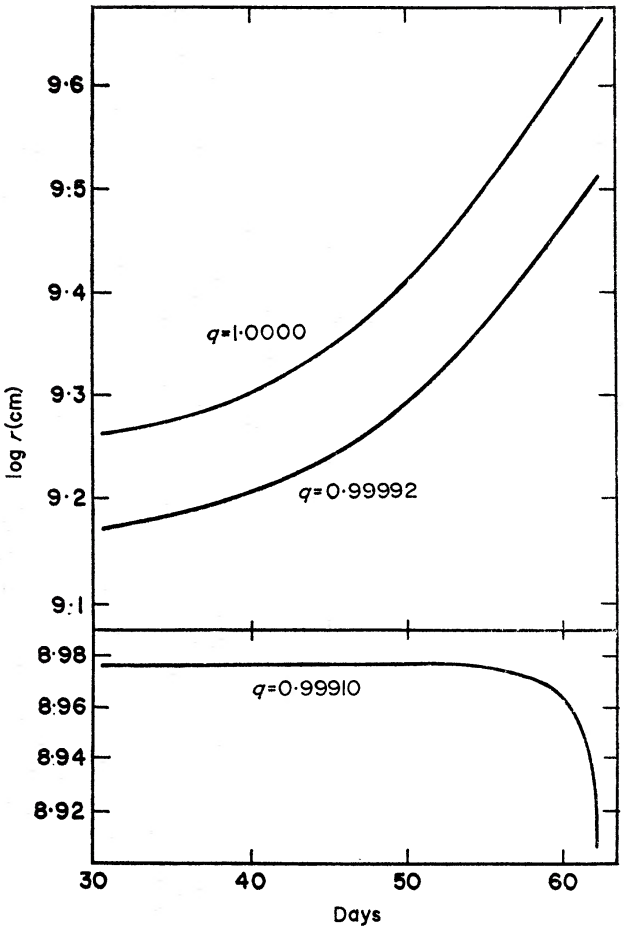

FIG. 4. *Radius as a function of time for three shells from the* $0{\cdot}5M_{\odot}$, $\log L/L_{\odot} = -1{\cdot}507$, $\log T_e = 4{\cdot}281$, *evolutionary sequence.*

TABLE VII

Evolution of the shell source at

$0{\cdot}5M_{\odot}$ $\log L/L_{\odot} = -1{\cdot}210$ $\log T_e = 4{\cdot}343$

Shell 40

Time (day)	log T	log ρ	log ϵ_{nuc}	log L	log r	log S	X_H	X_{He}
−6·4E3 (yr)	7·253	3·453	3·800	32·28	8·972	9·427	0·9000	0·0990
−1·6E2	7·672	3·040	8·860	34·827	8·981	9·480	0·8997	0·0993
+7·9	7·829	2·761	10·308	35·742	8·992	9·505	0·8997	0·0993
14·6	7·892	2·607	10·795	36·100	9·002	9·517	0·8996	0·0994
18·3	7·965	2·356	11·253	36·560	9·021	9·534	0·8993	0·0997
22·0	8·086	1·855	11·833	38·201	9·053	9·563	0·8983	0·1007

Shell 41

−6·4E3 (yr)	7·274	3·927	0·0	32·136	8·964	9·006	0·0	0·999
−1·6E2	7·246	3·885	0·0	−32·977	8·965	9·006	0·0	0·999
+7·9	7·219	3·844	0·0	−32·933	8·967	9·006	0·0	0·999
14·6	7·204	3·821	0·0	−32·854	8·968	9·006	0·0	0·999
18·3	7·191	3·802	0·0	−32·674	8·968	9·006	0·0	0·999
22·0	8·072	5·098	6·0	−39·200	8·901	9·006	0·0	0·999

(c) $\log L/L_\odot = -1{\cdot}210$, $\log T_e = 4{\cdot}343$

The evolution of this model is presented in Table VII and Fig. 5. It is similar to the previous model but more violent. Since heating by accretion was included in the model, the evolution time was reduced to 6400 years. A convective region was formed and gradually extended itself towards the surface. Core compression and helium burning also occurred in this model. However, the inward velocity of the core reached 10^4 cm s^{-1}—a factor of 10 higher than in the last model. Helium burning reached 10^6 erg g^{-1} s^{-1} and slowed down core compression and ended the evolution. As this model approached the peak of the outburst, it was producing 10^{45} erg hr^{-1}, and the total energy produced was 10^{47} erg. If one per cent of the 10^{47} erg can appear in the kinetic energy of the expanding shell, then this model has produced the energy released in the most energetic nova.

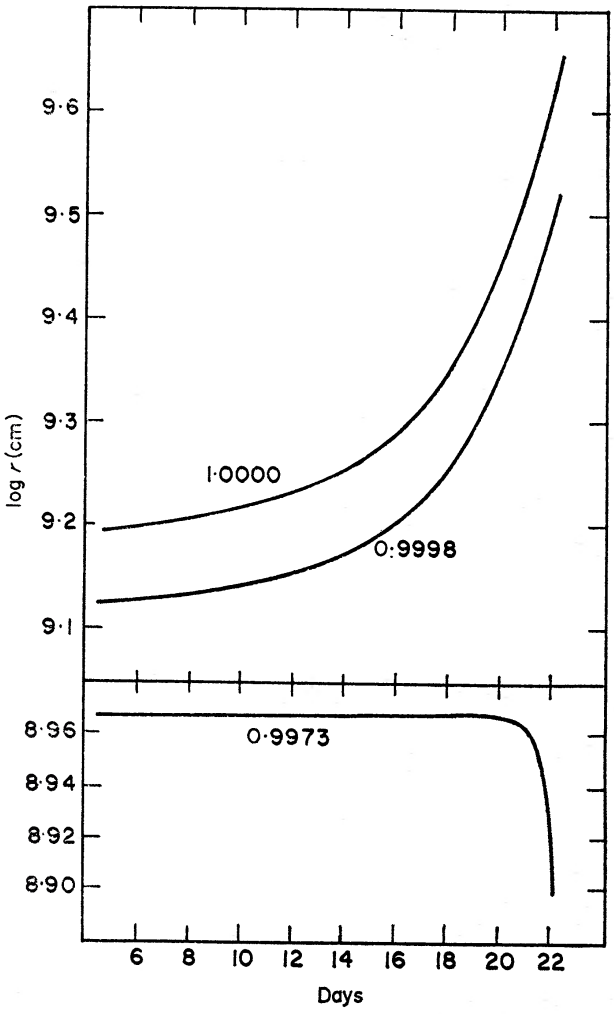

FIG. 5. *Radius as a function of time for three shells from the* $0{\cdot}5M_\odot$, $\log L/L_\odot = -1{\cdot}210$, $\log T_e = 4{\cdot}343$ *evolutionary sequence.*

5. SUMMARY AND DISCUSSION

These calculations show that a thermal runaway can occur in the envelope of a white dwarf and produce the energy observed in the outburst of a common nova. Schatzman's (1965) objections to this process are not correct because he neglected convection and the existence of an extensive non-degenerate region in the envelope

of a white dwarf. The conductivity of the degenerate electrons is unimportant in the region of the shell source and does not transport a significant amount of energy into the interior. In fact, the total amount of energy carried into the interior during the evolution of the $0{\cdot}12\ M_\odot$ model for DQ Her was sufficient to raise the temperature by only 1 °K. The heating observed in the layers of the core just below the shell source was caused by the adiabatic compression of these layers as the shell source expanded.

The results of the evolution of $0{\cdot}12\ M_\odot$ provide additional evidence for the existence of a shock-front at the surface of the white dwarf component of DQ Her. The luminosity and effective temperature derived for the star by Kraft (1959) resulted in evolutionary sequences that did not produce the energy observed during the nova outburst. When the existence of the shock-front was assumed, it was then possible to obtain a luminosity and effective temperature that resulted in a thermal runaway which liberated the same amount of energy as observed in the outburst of DQ Her.

An interesting feature of the evolution of these models is the compression of the layers of the core just beneath the shell source which occurs as the peak of the outburst is reached. The velocity of the compression (note the variation in time scale in Figs 3, 4 and 5) varies from model to model and appears to be dependent on the mass. The compression velocity in the sequence with $M = 0{\cdot}5\ M_\odot$, $L/L_\odot = -1{\cdot}210$, $\log T_e = 4{\cdot}343$, is a factor of a hundred greater than in the $0{\cdot}12 M_\odot$ sequence. In addition, the core compression reaches the point in both the $0{\cdot}5\ M_\odot$ sequences where helium burning is initiated at the edge of the core. Sparks (1969) has shown that two different kinds of ejections (shock and pressure) occur in the outburst of the common novae. Because the present calculations are hydrostatic, it is preliminary to associate the differences in the rates of core compression at different masses with his results. Calculations of the hydrodynamic evolution of these models is now in progress. It is also planned to carry the evolution to higher masses.

One last comment is to be made on the possible relationship between the common novae and recurrent novae. At $0{\cdot}5\ M_\odot$, $\dot{T}_{\rm tr}/T_{\rm tr} \approx 500\dot{M}/M$. If instead of the mass accretion rate of $10^{-8}\ M_\odot\ {\rm yr}^{-1}$, as proposed for DQ Her (Starrfield 1970), we assume that a $0{\cdot}5\ M_\odot$ white dwarf with $\log L/L_\odot = -1{\cdot}0$ is accreting $10^{-6}\ M_\odot\ {\rm yr}^{-1}$, in 50 years it will accrete 10^{29} g. The temperature rise, due to accretion, will be nearly a million degrees over the 12·6 million expected at a depth of 10^{29} g. While no $0{\cdot}5\ M_\odot$ model was evolved at this luminosity, comparison with the $0{\cdot}5\ M_\odot$ evolutionary sequences imply that it would have a thermal runaway but would not liberate as much energy. Models with larger mass should certainly have a thermal runaway at a luminosity of $\log L/L_\odot = -1{\cdot}0$.

ACKNOWLEDGMENTS

The work on $0{\cdot}12\ M_\odot$ was presented to the Graduate School of the University of California at Los Angeles in partial fulfillment of the requirements for the Ph.D. degree. The author gratefully acknowledges valuable discussions with Drs Edward Upton, Arthur Cox, Richard Larson, Rudolph Kippenhahn, James Hunter, Pierre Demarque, Stuart Pottasch, and Erik Zimmermann. He is also grateful to Drs Pierre Demarque and Richard Larson for reading and commenting on the manuscript. He received generous allotments of computer time from the Yale Computing

Facility, the U.C.L.A. Campus Computing Network, and the Institute for Space Studies. In addition, he would like to thank Dr L. Mestel for pointing out some historical errors in the original manuscript.

Yale University Observatory

Received in original form 1970 *October* 22

REFERENCES

Baker, N. & Kippenhahn, R., 1962. *Z. Astrophys.*, **54**, 114.
Bath, G. T., 1969. *Astrophys. J.*, **158**, 571.
Böhm-Vitense, E., 1958. *Z. Astrophys.*, **46**, 108.
Cox, A. N. & Stewart, J. N., 1965. *Astrophys. J. Suppl.*, **11**, 22.
Giannone, P. & Weigert, A., 1967. *Z. Astrophys.*, **67**, 41.
Hamada, T. & Salpeter, E. E., 1961. *Astrophys. J.*, **134**, 683.
Hazelhurst, J., 1962. *Adv. Astr. Astrophys.*, **1**, 1.
Hubbard, W. B. & Lampe, M., 1969. *Astrophys. J. Suppl.*, **18**, 297.
Iben, I., 1965. *Astrophys. J.*, **141**, 1015.
Kippenhahn, R., Thomas, H. C. & Weigert, A., 1965. *Z. Astrophys.*, **61**, 241.
Kippenhahn, R., Weigert, A. & Hofmeister, E., 1967. In *Methods in Computational Physics*, Vol. 7, ed. B. Alder, S. Fernbach, and M. Rotenberg, Academic Press, New York, p. 129.
Kraft, R. P., 1959. *Astrophys. J.*, **130**, 110.
Kraft, R. P., 1963. *Adv. Ast. Astrophys.*, **2**, 43.
Kraft, R. P., 1964. *Astrophys. J.*, **139**, 457.
Krzeminski, W., 1965. *Astrophys. J.*, **142**, 1051.
Lee, T. D., 1950. *Astrophys. J.*, **111**, 625.
Matsushima, S. & Terashita, Y., 1969. *Astrophys. J.*, **156**, 219.
Mestel, L., 1952. *Mon. Not. R. astr. Soc.*, **112**, 598.
Mumford, G. S., 1967. *Publ. astr. Soc. Pacif.*, **79**, 283.
Nather, R. E. & Warner, B., 1969. *Mon. Not. R. astr. Soc.*, **143**, 145.
Paczynski, B., 1965a. *Acta Astr.*, **15**, 89.
Paczynski, B., 1965b. *Acta Astr.*, **15**, 197.
Payne-Gaposchkin, E. & Gaposchkin, S., 1942. *Harvard Circ.*, No. 445.
Reeves, H., 1965. In *Stars and Stellar Systems*, Vol. 8, ed. L. H. Aller and D. B. McLaughlin, University of Chicago Press, Chicago, ii.
Rose, W. K., 1968. *Astrophys. J.*, **152**, 245.
Saslaw, W. C., 1968. *Mon. Not. R. astr. Soc.*, **138**, 337.
Schatzman, E., 1958. *White Dwarfs*, Interscience, New York.
Schatzman, E., 1965. In *Stars and Stellar Systems*, Vol. 8, ed. L. H. Aller and D. B. McLaughlin, University of Chicago Press, Chicago, vi.
Schwarzschild, M., 1958. *Structure and Evolution of the Stars*, Princeton University Press, Princeton.
Schwarzschild, M. & Härm, R., 1965. *Astrophys. J.*, **142**, 855.
Skilling, J., 1968. *Nature, Lond.*, **218**, 923.
Smak, J., 1969. *Acta Astr.*, **19**, 287.
Sparks, W., 1969. *Astrophys. J.*, **156**, 569.
Starrfield, S., 1970. *Astrophys. J.*, **161**, 361.
Tolman, R. C., 1938. *The Principles of Statistical Mechanics*, Oxford University Press, London, x.
Walker, M. F. & Chincarini, G., 1968. *Astrophys. J.*, **154**, 157.